OPAL Physics Note PN296

Measurement of the Muonic Branching Ratio of the τ.

The OPAL Collaboration

22nd July 1997

Abstract

The branching ratio of the $\tau \to \mu\nu\bar{\nu}$ decay mode has been measured with the OPAL detector to be $(17.48 \pm 0.12 \pm 0.08)\%$ where the first error is statistical and the second is systematic. The branching ratio, together with other measurements, has been used to test electron-muon and muon-tau universality in the charged current weak interaction at a 0.5% level of precision.

This note describes preliminary OPAL results to be submitted to the XVIII International Symposium on Lepton-Photon Interactions, Hamburg, 28 July - 1 August 1997

1 Introduction

The $\tau \to \mu\nu\bar{\nu}$ decay is an important probe of the Standard Model. The branching ratio, together with other measurements, can be used to determine the relative charged current couplings of the electron, muon and tau leptons. It has also been used to put constraints on the ν_τ mass and mixing [1]. OPAL has previously published a measurement of the $\tau \to \mu\nu\bar{\nu}$ branching ratio based on data recorded between 1990 and 1992 [2]. This paper describes an improved measurement which is based on a larger event sample (data recorded between 1991 and 1994) and which uses a different muon selection method designed to reduce the systematic error. In the new selection method, the muon chambers and the tracking chambers are used to isolate the main sample of $\tau \to \mu\nu\bar{\nu}$. In addition a restricted fiducial region, where the muon detection efficiency of both the calorimeters and the muon chambers is very high and uniform, is defined for the analysis. An independent muon sample is selected using the calorimeters and this allows the efficiency of the main muon selection to be determined from the data.

A full description of the OPAL detector can be found in reference [3]. Here we describe those aspects of the detector [1] which are particularly relevant to the present measurement. The central tracking chambers measure the momenta of charged particles in a uniform magnetic field. A precision vertex chamber is surrounded by a large-volume jet drift chamber divided into 24 azimuthal sectors, where charge deposited on each wire provides a measurement of the energy loss dE/dx of charged particles in the chamber. In the barrel region, the jet chamber is surrounded by drift chambers which measure the z-coordinates of charged particles as they leave the jet chamber. The magnetic coil and pressure vessel of the central tracking chambers are surrounded by a time-of-flight(TOF) counter array and an electromagnetic calorimeter (ECAL) consisting of 9440 lead-glass blocks with a presampler. The instrumented return yoke serves as a hadron calorimeter (HCAL) and muon tracker and is surrounded by four layers of (MUON) drift chambers.

The τ pair Monte Carlo samples were generated using the KORALZ 4.0 package [4]. The dynamics of the τ decays were simulated with the TAUOLA 2.0 decay library [5]. The Monte Carlo events were then passed through the GEANT simulation [6] of the OPAL detector [7] that treats in detail the detector geometry and material, as well as effects of detector resolution and efficiencies.

The τ pair event selections are very similar to those used in the previous OPAL measurement of this branching ratio. We describe here the procedures used to make the branching ratio measurements and outline how backgrounds and efficiencies and their corresponding systematic errors are determined from Monte Carlo events and data control samples.

[1] A right-handed coordinate system is used. The x-axis points towards the centre of the LEP ring, the y-axis upwards and the z-axis in the direction of the electron beam. The polar angle θ and the azimuthal angle ϕ are defined with respect to the z-axis and x-axis, respectively.

2 Selection of events

At LEP, τ pair events can be clearly identified because the large relativistic boost means that the decay products are highly collimated. For an event to be considered in the $e^+e^- \to \tau^+\tau^-$ preselection the detectors in the barrel region are required to be fully operational. For this analysis, a geometric region is chosen in which both the hadron calorimeter and the muon barrel detectors have a very high efficiency. This reduces the available statistics but reduces significantly the systematic error in the analysis.

2.1 $e^+e^- \to \tau^+\tau^-$

The selection of $e^+e^- \to \tau^+\tau^-$ events is made by first rejecting beam - gas, cosmic ray and other backgrounds and then rejecting multihadronic and two photon events as described below. After this preselection, only lepton pair events should remain and at this stage the $e^+e^- \to e^+e^-$ and $e^+e^- \to \mu^+\mu^-$ events are rejected. In selecting τ pair events and in identifying τ decay channels, both charged tracks and electromagnetic clusters, where a cluster is defined as a group of contiguous lead-glass blocks which has a minimum energy of 100 MeV, are considered.

A charged track must have a minimum momentum transverse to the beam of 100 MeV/c, a measured $|d_0| < 2$ cm, and a measured $|z_0| < 75$ cm, where $|d_0|$ is the distance of closest approach of the track to the beam axis, and $|z_0|$ is the displacement along the beam axis from the nominal interaction point at the point of closest approach to the beam. The track must also have at least 20 measured space points in the jet chamber and at least one point within 75 cm of the beam axis.

The multihadron background is reduced by requiring between 2 and 6 charged tracks and excluding events with more than 10 electromagnetic clusters. Cosmic ray backgrounds are suppressed by requiring at least one charged track with a measured $|d_0| < 0.5$ cm and a measured $|z_0| < 20$ cm, and requiring the magnitude of the average z of all tracks at their points of closest approach to the beam to be less than 20 cm. In addition, there must be at least one TOF signal within 10 ns of the nominal expected value. An event is rejected if all pairs of TOF signals separated by more than 165° in azimuth have time differences greater than 10 ns.

Using a jet finding algorithm, charged tracks and clusters are grouped together in cones of half-angle 35° [8]. A candidate lepton pair event must have exactly two cones, and each cone must contain at least one charged track. All the tracks and clusters inside each cone form a jet. The visible energy of each jet is taken as the scalar sum of the track momenta or the electromagnetic cluster energy associated with that jet whichever is the larger. Only jets with visible energy greater than 1% of the beam energy are accepted. The direction of the jet is calculated from the momentum sums of the tracks and clusters in the cone. The average value of $|\cos\theta|$ for the two jets must be less than 0.68.

A restricted barrel region of the OPAL detector is defined in which less efficient zones of the calorimeters and muon detectors are omitted. Within the selected region, muons will be detected with high efficiency by both of these detectors. The most energetic track in at least one of the candidate tau decay cones must be in this restricted barrel region. This avoids the detector's support structures, the strips in ϕ where the hadron calorimeter sectors are joined and also the edges of each hadron calorimeter sector. It also excludes small regions around the anode planes of the tracking chambers, as the reconstruction of position and momentum in these regions is less precise and not well modelled by the Monte Carlo. The τ pair selection efficiency in the resulting restricted barrel region is 93% and the muon identification efficiency is around 90%, for either the muon chamber or the calorimeter algorithm.

To remove backgrounds due to two-photon processes, the acollinearity of the two jets is required to be less than 15°. Rejection of residual two-photon backgrounds exploits the low visible energies and very low transverse momenta typical of $e^+e^- \to (e^+e^-)X$ events. An event is rejected if the sum of visible energies of the jets is less than 3% of the collision energy ($E_{\rm CM}$). Further, if the total visible energy is less than 20% of $E_{\rm CM}$, the event is rejected if the missing transverse momenta, calculated separately for charged tracks and for electromagnetic clusters, are both less than 2 GeV/c.

The $e^+e^- \to e^+e^-$ background in the $\tau^+\tau^-$ sample is reduced substantially by requiring that events satisfy either $\sum E_{\rm cls} \leq 0.8\ E_{\rm CM}$ or $(\sum E_{\rm cls} + 0.3 \sum p_{\rm trk}) \leq E_{\rm CM}$, where $\sum E_{\rm cls}$ is the total energy deposited in the lead-glass calorimeter and $\sum p_{\rm trk}$ is the total momentum of the charged tracks [8]. Muon pair events are removed by rejecting events where both cones contain a particle identified as a muon by the electromagnetic or hadronic calorimeter or muon chambers as detailed in [2], and the scalar sum of the highest energy cluster and the highest momentum track when summed over both cones is greater than $0.6\ E_{\rm CM}$. These cuts to remove $e^+e^- \to e^+e^-$ and $e^+e^- \to \mu^+\mu^-$ events are the same as used in [8].

After these selections the remaining background in the τ pair sample is predicted by Monte Carlo to be around 1% as presented for each of the three different data samples in table 1. These initial background estimates and errors are corrected using control samples from the data as described in section 4.1.

2.2 Selection of $\tau \to \mu\nu\bar{\nu}$

In order to isolate the sample of $\tau \to \mu\nu\bar{\nu}$ decays used for the branching ratio measurement, muon identification cuts are made which only use information from the tracking and muon chambers. Each cone must contain one charged track and it must be in the restricted barrel acceptance region discussed in the previous section. In this cone there must be a track segment reconstructed independently in the muon chambers. The positional separation variable, $\chi_{\rm pos}$, for the significance of the measured separation between this muon segment and the extrapolated position of the charged particle as measured in the tracking chambers, must not exceed 3. There is reasonable agreement between the $\chi_{\rm pos}$ distributions for data and Monte Carlo, as shown in figure 1(a).

In order to further suppress muon-pair background in the $\tau \to \mu\nu\bar{\nu}$ sample, where one muon has not been identified, a cut on a momentum variable is included. The quantity

$$x_\mu = \frac{(p_{\mathrm{trk}} + E_{\mathrm{cls}} - 0.5\ \mathrm{GeV})}{\mathrm{E_{beam}}}$$

is defined, where p_{trk} is the momentum of the track, E_{cls} is the energy of the ECAL cluster associated with the track (to include radiative muon pairs), E_{beam} is the beam energy, and the 0.5 GeV is subtracted to account for the average deposition made by a minimum-ionising particle in the electromagnetic calorimeter. The x_μ distribution of the nearside cone, when the farside cone has $x_\mu > 0.9$, is shown for data and Monte Carlo in figure 1(b) . These distributions agree well with each other and the enhancement for x_μ in the nearside cone above 0.9 indicates a residual background of dimuon events in the sample. Therefore events where x_μ in both cones exceed 0.9 are rejected.

Low momentum muons are ranged out by the calorimeter and the cutoff momentum varies with the $\cos\theta$ of the particle. In order to reduce any sensitivity to the modelling of this effect a minimum x_μ of 0.05 is required for the $\tau \to \mu\nu\bar{\nu}$ candidates.

After these selections the remaining background in the $\tau \to \mu\nu\bar{\nu}$ sample is predicted by Monte Carlo to be around 2%. These results are presented for each of the three different data samples in table 2. These initial background estimates and errors are corrected using control samples from the data as described in section 4.2.

2.3 Selection of $\tau \to \mu\nu\bar{\nu}$ control sample

The $\tau \to \mu\nu\bar{\nu}$ selection efficiency using the muon chambers described in the last section is initially estimated from Monte Carlo. However, the efficiency of this selection for both data and Monte Carlo is measured in this analysis by using a largely independent $\tau \to \mu\nu\bar{\nu}$ selection using the electromagnetic and hadronic calorimeters. Since the $\tau \to \mu\nu\bar{\nu}$ selection utilises only the muon chambers and the tracking chambers, this independent selection of high purity and efficiency can be used to evaluate the performance of the Monte Carlo.

The selection cuts for this calorimeter based $\tau \to \mu\nu\bar{\nu}$ control sample are now described. There must be one charged track in the cone and it must lie in the restricted barrel acceptance region. There must be at least one hit in the three outermost hadron calorimeter layers. The importance of this cut in reducing the background is illustrated in figure 1(c). In addition, the average number of hadron calorimeter hits per hit layer is required to be less than 3. In order to reduce further the non $\tau \to \mu\nu\bar{\nu}$ contribution, the electromagnetic calorimeter energy associated with the candidate track must be less than 1.5 GeV. The invariant mass of the combination of the charged track (assuming the pion mass) and the electromagnetic energy detected in the cone (assuming the photon mass), less 0.5 GeV to account for the average energy deposition of the muon, is calculated. A requirement that this invariant mass be less than 0.3 GeV removes a substantial $\tau \to \rho\nu$ contribution. Finally, to minimise any differences in the momentum spectra of the two muon samples, events with $x_\mu > 0.9$ in both cones are rejected and the x_μ of the candidate must exceed 0.05.

This control sample has a muon detection efficiency of around 90%, similar to the primary muon sample, and the non-muon background in this sample is predicted to be around 1.5%. The background level for the muon chamber selection is slightly higher than this but it is chosen for the main analysis because the systematic errors are smaller using this sample.

3 $\tau \to \mu\nu\bar{\nu}$ Selection Efficiency

The initial efficiency measurement of the $\tau \to \mu\nu\bar{\nu}$ muon chamber selection is made using Monte Carlo samples and the results are presented in table 3. However, this efficiency is corrected using the $\tau \to \mu\nu\bar{\nu}$ control data sample selected using the calorimeters. This procedure is now described and the corrected efficiency results are then presented.

3.1 Independence of the two $\tau \to \mu\nu\bar{\nu}$ samples

The track requirement and the cuts on x_μ are the only common selections used in isolating samples of $\tau \to \mu\nu\bar{\nu}$ decays with the muon chambers and with the calorimeters. If these samples are independent then the product of the efficiency of each sample should equal the efficiency obtained by applying both selections simultaneously. This means that $\epsilon_{\rm b} = \epsilon_{\rm m}\epsilon_{\rm c}$ where $\epsilon_{\rm b}$ is the efficiency for selecting $\tau \to \mu\nu\bar{\nu}$ using both algorithms, $\epsilon_{\rm m}$ using the muon chamber selection and $\epsilon_{\rm c}$ using the calorimeter selection. Any correlation can be assessed by calculating a ratio, F, defined as: $\frac{\epsilon_{\rm b}}{\epsilon_{\rm m}\epsilon_{\rm c}}$ which will equal one if the selections are independent. In this analysis we expect a small correlation, because of the common track requirements, but it is important to check that the size and momentum dependence of any correlation is well reproduced by the Monte Carlo.

Samples of dimuons and two-photon muon pairs from data and Monte Carlo are selected as described in [2] and used to study the correlation factor F at the two extremes of the momentum spectrum. For this study the cut $x_\mu > 0.9$ for both muons is removed for the muon-pair samples. The τ pair Monte Carlo is used to study muons over the full momentum range. The results for the efficiencies of the calorimeter and muon chamber selections and F are listed in table 4. The efficiency of the muon chamber algorithm is somewhat higher than that of the calorimeter algorithm for muon pairs because radiative events can fail the requirement of small energy deposit in the electromagnetic calorimeter. For the low momentum muons from the two photon samples the calorimeter algorithm has a slightly higher efficiency. These efficiency measurements and correlation factors are consistent between data and Monte Carlo for each sample and the correlation factor is close to one in both samples.

There is a small positive correlation observed in all samples which is presumably due to the common track element in the selections. The results for the τ pair Monte Carlo sample yield similar results to those obtained at the two extremes of the muon momentum spectrum. The variation of F with momentum is also measured with this sample and no significant momentum dependent effects are observed.

We conclude from this study that the efficiency correction for the muon chamber selection can be determined reliably from the calorimeter selected data sample. No significant difference in correlation factor between data and Monte Carlo has been observed.

3.2 Correcting the Efficiency

The correction to the efficiency of the muon chamber sample is made as follows. The calorimeter muon selection is applied to τ pair events from data and Monte Carlo to produce samples of $\tau \to \mu\nu\bar{\nu}$ candidates of high purity. These samples are then used as input to the muon chamber selection and the resulting efficiencies for data and Monte Carlo are compared. A correction factor, C_{eff}, is defined as

$$C_{\text{eff}} = \frac{\left[\frac{\text{Number of cones passing muon chamber and } \mathrm{H_{CAL}} \text{ selections}}{\text{Number of cones passing } \mathrm{H_{CAL}} \text{ selection}}\right]^{\text{Data}}}{\left[\frac{\text{Number of cones passing muon chamber and } \mathrm{H_{CAL}} \text{ selections}}{\text{Number of cones passing } \mathrm{H_{CAL}} \text{ selection}}\right]^{\text{MC}}}.$$

As the measurement is made with a sample of $\tau \to \mu\nu\bar{\nu}$ decays the calculated efficiency has the appropriate momentum weighting.

A number of checks of this method were made. Firstly, to check that the background in the calorimeter muon sample is sufficiently well modelled by Monte Carlo, several of the cuts were relaxed in order approximately to double the predicted background. This resulted in a negligible change to C_{eff}. The efficiency correction factor C_{eff} as a function of x_μ as determined from the complete data and Monte Carlo samples is shown in figure 2. The correction factor is close to 1 over the full range of x_μ and there is no significant x_μ dependence observed.

The predicted efficiency, the correction factor determined from the data and the final corrected value of the efficiency are shown for each of the three data samples in table 3. The corrected efficiency is approximately 90% in all three data samples.

4 Backgrounds

The residual background fractions in the $e^+e^- \to \tau^+\tau^-$ and $\tau \to \mu\nu\bar{\nu}$ samples are initially estimated from Monte Carlo studies, with full detector simulation, of $e^+e^- \to e^+e^-$ [9], $e^+e^- \to \mu^+\mu^-$ [4], $e^+e^- \to q\bar{q}$ [10], $e^+e^- \to (e^+e^-)X$ [11] and all decay modes of the reaction $e^+e^- \to \tau^+\tau^-$ [4]. The backgrounds estimated from Monte Carlo are compared with those obtained from background enhanced samples of data for each of the three different data samples using the procedure described in [2]. The ratio of the numbers of events from data and Monte Carlo for a particular background source is used to correct the predicted background level. The error on the correction factor is taken as either the statistical error on the ratio, or as half the deviation from unity of the central value, whichever is the greater.

4.1 Measurement of Background in τ pair sample

The τ pair background Monte Carlo estimates are shown for each of the three samples in table 1. The total background is estimated at much less than 1% except for the 1994 Monte Carlo sample where the multihadronic background contribution is 1.1%. This higher estimate has also been identified in other analyses which have used this sample. However, the use of data control samples allows this background and other initial Monte Carlo estimates of background to be modified suitably as discussed below. The corrected background estimates are also included in table 1.

In this analysis, where the jet chamber anode plane regions are excluded, the muon-pair contamination is typically 0.1% which is very much lower than in the previous analysis [2]. The accuracy of the prediction of the muon-pair background remaining in the τ pair pair sample is assessed by comparing the number of data and Monte Carlo events with both cones identified as muons by either calorimeter or muon chambers. The scalar sum of the highest energy cluster and the highest momentum track of both cones is also required to be between 0.6 and 0.75 E_{CM} . Using this control sample, the muon-pair background estimate and its error are both increased.

The modelling of the multihadronic background was tested by relaxing the multiplicity cut in the event selection to include up to eight tracks and comparing the number of data and Monte Carlo events with topologies 2-4, 2-6, 3-4 and 4-4. The results show that the Monte Carlo estimates, which included a significantly higher value for the 1994 sample due to the inclusion of B** in the modelling of B decays, are corrected to values which are reasonably consistent between the three data samples.

The level of two photon backgrounds were assessed by comparing the number of data and Monte Carlo events which have acollinearity angle between 15° and 25° and have x_μ < 0.2 in each cone. Control samples of $e^+e^- \to (e^+e^-)\mu^+\mu^-$ and $e^+e^- \to (e^+e^-)e^+e^-$ are separated cleanly by also using the $d\mathrm{E}/dx$ information for the track in each cone. The $d\mathrm{E}/dx$ of the track in each cone is required to be less than 8.5 keV/cm for $e^+e^- \to (e^+e^-)\mu^+\mu^-$ and greater than 9.5 keV/cm for $e^+e^- \to (e^+e^-)e^+e^-$. The correction factors for all the data samples are close to unity and consistent between the various data samples.

The background in the τ pair sample due to $e^+e^- \to e^+e^-$ is checked by comparing the number of events with total cluster energy between 0.7 and 0.9 E_{CM} in the data with that observed in the Monte Carlo. These samples are dominated by $e^+e^- \to e^+e^-$ events and allow the Monte Carlo prediction to be checked with data in a region close to the cut used to select the τ pair sample. The $e^+e^- \to e^+e^-$ background estimates for two of the data sets are increased as a result of this study and the errors on these estimates are also increased.

After the corrections described in this section the overall background in the τ pair sample for the three data samples is estimated to be $(1.10\pm0.16)\%$, $(1.21\pm0.18)\%$ $(1.09\pm0.29)\%$. There is good agreement between these τ pair background measurements for the three different data sets.

4.2 Measurement of Background in $\tau \to \mu\nu\bar{\nu}$ sample

The Monte Carlo predictions of background and the corresponding corrected values for the data from each year are listed in table 2. The selections applied to isolate the control samples are now described.

The dominant background to the $\tau \to \mu\nu\bar{\nu}$ decay is from hadronic τ decays, particularly $\tau \to \pi(\mathrm{K})\nu$ and $\tau \to \rho\nu$. To evaluate the corrected contribution of hadronic τ decay background, a ρ-recognition algorithm is used [12]. To reduce further the $\tau \to \mu\nu\bar{\nu}$ contribution in this sample, it is also required that the number of lead-glass blocks in the highest-energy cluster in the cone exceeds 9. The selection is based upon calorimeter information and so is independent of the muon-chamber-based $\tau \to \mu\nu\bar{\nu}$ selection. The predicted composition of the selected sample is $\tau \to \rho\nu$ (75%), $\tau \to \pi\nu$ (20%) with $< 0.1\%$ of $\tau \to \mu\nu\bar{\nu}$ decays.

The predicted muon-pair background in the $\tau \to \mu\nu\bar{\nu}$ sample is much smaller than that from hadronic tau decays. To be included in the muon-pair control sample, the highest momentum track and highest energy cluster, when summed over both cones, must exceed 0.7 E_{CM} with the cones colinear within $0.4°$ and the track in the opposite cone must be identified as a muon with $x_\mu > 0.8$. The correction factors are close to unity for all the data samples.

Finally the $e^+e^- \to (e^+e^-)\mu^+\mu^-$ Monte Carlo background estimate was checked with a sample selected to include one charged track per cone (each with $x_\mu < 0.5$), acolinearity $> 10°$ and a muon candidate in the opposite cone satisfying the muon chamber selection with $\chi_{\mathrm{pos}} < 3.0$. The agreement between data and Monte Carlo was good for all data sets.

The corrected $\tau \to \mu\nu\bar{\nu}$ background estimates discussed in this section are all summarised in table 2. There is very little variation in any of these background estimates for the three different data samples.

5 Branching Ratio Results

The branching ratio is calculated from the following expression:

$$B(\tau \to \mu\nu\bar{\nu}) \quad \equiv \quad \frac{N_{Cand}^{\tau\to\mu\nu\bar{\nu}}}{N_{Cand}^{\tau}} \cdot \frac{(1 - f_{Bkgd}^{\tau\to\mu\nu\bar{\nu}})}{(1 - f_{Bkgd}^{\tau})} \cdot \frac{1}{\epsilon^{\tau\to\mu\nu\bar{\nu}}} \cdot \frac{1}{F_{Bias}^{\tau\to\mu\nu\bar{\nu}}}$$

The number of $\tau \to \mu\nu\bar{\nu}$ candidates is $N_{Cand}^{\tau\to\mu\nu\bar{\nu}}$ and N_{Cand}^{τ} is the number of τ candidates. The estimated background fraction in the $\tau \to \mu\nu\bar{\nu}$ sample from other τ decay modes and non-τ sources (table 2) is $f_{Bkgd}^{\tau\to\mu\nu\bar{\nu}}$ and the estimated background of non-τ events in the τ pair sample is f_{Bkgd}^{τ} (table 1). The corrected efficiency for selecting $\tau \to \mu\nu\bar{\nu}$ decays from the selected τ pairs is $\epsilon^{\tau\to\mu\nu\bar{\nu}}$ (table 3). The relative enhancement for detecting $\tau \to \mu\nu\bar{\nu}$ decays with respect to other τ decay modes is $F_{Bias}^{\tau\to\mu\nu\bar{\nu}}$. The branching ratio (BR) for $\tau \to \mu\nu\bar{\nu}$ is determined from Monte Carlo before and after the $\tau\tau$ selection is made and

$F_{Bias}^{\tau\to\mu\nu\bar{\nu}}$ is defined as the ratio (true BR in selected $\tau\tau$ sample)/ (true BR in generated $\tau\tau$ sample). The values of all of these quantities are given for each year in table 5.

Using the data and Monte Carlo from each of the three independent samples 1991-92, 1993 and 1994, the above expression is used to calculate the $\tau \to \mu\nu\bar{\nu}$ branching ratio. The three results are shown in table 5 and a breakdown of the various error contributions associated with the result from each year is given in table 6, where it is clear that the statistical errors dominate. The procedure used to estimate the systematic error contributions for the τ pair and $\tau \to \mu\nu\bar{\nu}$ backgrounds using control samples from the data have been described in section 4. The systematic error for $F_{Bias}^{\tau\to\mu\nu\bar{\nu}}$ has been estimated by measuring the sensitivity of this quantity to smearing of the Monte Carlo momentum and energy with a range of different resolutions and includes a contribution from Monte Carlo statistics. The error on the corrected efficiency includes a contribution from the statistics of the final data sample, which has been included in the statistical error, and one from Monte Carlo statistics which is given separately in table 6. These errors are independent, so that they can be added in quadrature to produce the correct overall error for the efficiency.

The results from the three data samples are consistent with each other and the systematic error estimate is similar in each case. The Monte Carlo statistics contributions to these errors are independent for each sample but there are significant correlations between some of the other systematic errors for each data set. For the final error estimate we have made the conservative assumption that the systematic errors are fully correlated between the three data sets and taken the average of these systematic errors for the final result. The weighted average for the full data set is quoted as the final result. The final measured branching ratio value is:

$$B(\tau \to \mu\nu\bar{\nu}) = (17.48 \pm 0.12 \pm 0.08)\%$$

where the first error is statistical and the second systematic.

6 Discussion and Summary

The $\tau \to \mu\nu\bar{\nu}$ branching ratio has been measured to be $(17.48 \pm 0.12 \pm 0.08)\%$ using data recorded by the OPAL detector from 1991 to 1994. This result is consistent with and is significantly more precise than the previous OPAL result based on data recorded up until 1992 [2], of (17.48±0.18±0.23)%. This is due both to improved statistics and also to the use of an independent $\tau \to \mu\nu\bar{\nu}$ data sample which has allowed a significant reduction in the systematic errors. This measurement is consistent with the world average value [13] of (17.35±0.10)% and with the result of (17.31±0.12)% obtained by the ALEPH experiment [14] which is currently the most precise result from a single experiment. The error on this new OPAL result is comparable to the best achieved in a single experiment for this branching ratio.

The $\tau \to \mu\nu\bar{\nu}$ branching ratio can be used to test charged current lepton universality.

The ratio of widths for the decays $\tau \to \mu\nu\bar{\nu}$ and $\tau \to e\nu\bar{\nu}$ is related to g_μ/g_e[15]

$$\frac{\Gamma(\tau \to \mu\nu\bar{\nu})}{\Gamma(\tau \to e\nu\bar{\nu})} = \frac{g_\mu^2}{g_e^2}\frac{f(m_\mu^2/M_\tau^2)}{f(m_e^2/M_\tau^2)}$$

where g_μ and g_e are the charged current coupling constants for the muon and electron, and $f(x) = 1 - 8x + 8x^3 - x^4 - 12x^2 ln(x)$ is the phase space term due to final state particles having finite mass. Using the latest measurement of the τ mass by the BES collaboration of $1776.96^{+0.015+0.026}_{-0.014-0.018}$ MeV/c^2[16] and the OPAL $\tau \to e\nu\bar{\nu}$ branching ratio of $(17.78 \pm 0.10 \pm 0.09)\%$ [17], we obtain $g_\mu/g_e = 1.005 \pm 0.005$. These results for tau decay (which involves vector and axial vector currents) are in agreement with the even more precise results of [18] which show universality of the axial current. If this universality is assumed, the $\tau \to e\nu\bar{\nu}$ [17] and $\tau \to \mu\nu\bar{\nu}$ branching ratios from this measurement can be combined, after correcting for the difference in electron and muon masses, to produce a combined OPAL measurement of the τ electronic branching ratio of $\overline{B_e} = (17.88 \pm 0.10)\%$

A test of muon-tau universality can be made by comparing the partial widths for the decays of the tau and muons into electrons, which have the form [15]

$$\frac{g_\tau^2}{g_\mu^2} = 0.9996\frac{\tau_\mu}{\tau_\tau}\left[\frac{M_\mu}{M_\tau}\right]^5 \overline{B}(\tau \to e\nu\bar{\nu})$$

Using the OPAL τ-lifetime measurement of $(289.2 \pm 1.7 \pm\ 1.2) fs$ [19] we obtain $g_\tau/g_\mu = 1.005 \pm 0.005$. The OPAL tau lifetime and $\overline{B_e}$ measurements are shown on figure 3. The band is the Standard Model prediction assuming lepton universality and the width of the band corresponds to the uncertainty in the tau mass.

In conclusion the $\tau \to \mu\nu\bar{\nu}$ branching ratio has been measured to be $17.48 \pm 0.12 \pm 0.08$ using data recorded by the OPAL detector from 1991 to 1994 and is consistent with other measurements of this quantity. This result supersedes previous OPAL measurements of this branching ratio using only a subset of these data. The results have been used, together with other measurements, to test electron-muon and muon-tau charged current universality at a level of 0.5%.

References

[1] J.Swain, L.Taylor, Phys. Rev. **D55** (1997) 1.

[2] The OPAL Collaboration, R.Akers *et al.,* Z. Phys. **C66** (1995) 543.

[3] The OPAL collaboration, K. Ahmet *et al.*, Nucl. Instr. and Meth. **A305** (1991) 275.

[4] S. Jadach, B. F. L. Ward, and Z. Was, Comp. Phys. Comm. **79** (1994) 503; (KORALZ, Version 4.0).

[5] S. Jadach, J. H. Kühn, and Z. Was, Comp. Phys. Comm. **76** (1993) 361; (TAUOLA, Version 2.0).

[6] R.Brun *et al.*, GEANT3, Report DD/EE/84-1, CERN (1989).

[7] J.Allison *et al.*, Comp. Phys. Comm. **47** (1987) 55.

[8] The OPAL Collaboration, G. Alexander *et al.*, Phys. Lett. **B266** (1991) 201.

[9] M. Böhm, A. Denner and W. Hollik, Nucl. Phys. **B304** (1988) 687;
F.A. Berends, R. Kleiss, W. Hollik, Nucl. Phys. **B304** (1988) 712; (BABAMC).

[10] T. Sjöstrand, Comp. Phys. Comm. **39** (1986) 347;
T. Sjöstrand, Comp. Phys. Comm. **43** (1987) 367;
T. Sjöstrand, CERN-TH-6488/92.; (JETSET, Version 7.3)

[11] R. Bhattacharya, J. Smith, G. Grammer, Phys. Rev. **D15** (1977) 3267;
J. Smith, J.A.M. Vermaseren, G. Grammer, Phys. Rev. **D15** (1977) 3280.
(Vermaseren, Version 1.01)

[12] The OPAL Collaboration, G. Alexander *et al.* , Zeit. f. Physik **C72** (1996) 389-398.

[13] Particle Data Group, *Review of Particle Physics*, Phys. Rev. **D54** (1996), 1.

[14] The ALEPH Collaboration, D. Buskulic *et al.*, Z. Phys. **C70** (1996), 561.

[15] W. J. Marciano and A. Sirlin, Phys. Rev. Lett. **61** (1988) 1815.

[16] BES Collaboration, J.Z.Bai *et al.,* SLAC Preprint SLAC-PUB-6930.

[17] The OPAL Collaboration, G. Alexander *et al.* , Phys. Lett. **B369** (1996), 163.

[18] D.Britton *et al.,* Phys. Rev. Lett. **68** (1992) 3000;
G.Czapek *et al.,* Phys. Rev. Lett. **70** (1993) 17.

[19] The OPAL Collaboration, G. Alexander *et al.*, Phys. Lett. **B374** (1996) 341.

Background Reaction	Monte Carlo Predicted Background(%)	Corrected Background(%)
	1991-92	
$e^+e^- \to \mu^+\mu^-$	0.13 $\pm$0.01	0.20 $\pm$0.05
$e^+e^- \to q\bar{q}$	0.29 $\pm$0.04	0.51 $\pm$0.13
$e^+e^- \to (e^+e^-)\mu^+\mu^-$	0.05 $\pm$0.01	0.06 $\pm$0.02
$e^+e^- \to (e^+e^-)e^+e^-$	0.08 $\pm$0.02	0.08 $\pm$0.03
$e^+e^- \to e^+e^-$	0.15 $\pm$0.03	0.24 $\pm$0.07
Total		1.10 $\pm$ 0.16
	1993	
$e^+e^- \to \mu^+\mu^-$	0.12 $\pm$0.01	0.32 $\pm$0.10
$e^+e^- \to q\bar{q}$	0.19 $\pm$0.04	0.30 $\pm$0.08
$e^+e^- \to (e^+e^-)\mu^+\mu^-$	0.05 $\pm$0.01	0.07 $\pm$0.01
$e^+e^- \to (e^+e^-)e^+e^-$	0.09 $\pm$0.01	0.12 $\pm$0.02
$e^+e^- \to e^+e^-$	0.20 $\pm$0.02	0.42 $\pm$0.12
Total		1.21 $\pm$ 0.18
	1994	
$e^+e^- \to \mu^+\mu^-$	0.11 $\pm$0.01	0.18 $\pm$0.04
$e^+e^- \to q\bar{q}$	1.13 $\pm$0.01	0.55 $\pm$0.29
$e^+e^- \to (e^+e^-)\mu^+\mu^-$	0.06 $\pm$0.01	0.07 $\pm$0.01
$e^+e^- \to (e^+e^-)e^+e^-$	0.09 $\pm$0.01	0.09 $\pm$0.01
$e^+e^- \to e^+e^-$	0.22 $\pm$0.01	0.20 $\pm$0.02
Total		1.09 $\pm$ 0.29

Table 1: Estimated background fractions in the selected τ pair candidate events for the three different data sets before and after applying corrections based on data control samples. The latter are discussed in section 4.1.

Reaction	Monte Carlo Predicted Background (%)	Data-Corrected Background (%)
	1991-92	
$\tau \to \pi(\mathrm{K})\nu$	0.84	1.12 $\pm$0.25
$\tau \to \rho\nu$	0.80	1.07 $\pm$0.24
$e^+e^- \to \mu^+\mu^-$	0.17	0.17 $\pm$0.03
$e^+e^- \to (e^+e^-)\mu^+\mu^-$	0.28	0.29 $\pm$0.01
Total	2.10 $\pm$ 0.08	2.65 $\pm$ 0.37
	1993	
$\tau \to \pi(\mathrm{K})\nu$	0.70	0.90 $\pm$0.28
$\tau \to \rho\nu$	0.77	1.00 $\pm$0.31
$e^+e^- \to \mu^+\mu^-$	0.13	0.13 $\pm$0.02
$e^+e^- \to (e^+e^-)\mu^+\mu^-$	0.28	0.28 $\pm$0.01
Total	1.88 $\pm$ 0.08	2.31 $\pm$ 0.45
	1994	
$\tau \to \pi(\mathrm{K})\nu$	0.87	1.14 $\pm$0.21
$\tau \to \rho\nu$	0.74	0.98 $\pm$0.18
$e^+e^- \to \mu^+\mu^-$	0.13	0.12 $\pm$0.01
$e^+e^- \to (e^+e^-)\mu^+\mu^-$	0.26	0.25 $\pm$0.01
Total	1.99 $\pm$ 0.06	2.49 $\pm$ 0.29

Table 2: Estimated backgrounds in the selected $\tau \to \mu\nu\bar{\nu}$ candidate events before and after applying corrections using systematic studies discussed in the text. The corrections are discussed in Section 4.2

	91-92	93	94
MC efficiency (%)	86.53 $\pm$ 0.20	88.97 $\pm$ 0.18	90.92 $\pm$ 0.12
Correction factor	1.035 $\pm$ 0.015	1.020 $\pm$ 0.017	0.983 $\pm$ 0.011
Corrected efficiency (%)	89.54 $\pm$ 1.28	90.78 $\pm$ 1.56	89.41 $\pm$ 1.01

Table 3: Selection efficiencies (%) for the selection of $\tau \to \mu\nu\bar{\nu}$ as predicted from Monte Carlo and corrected for this analysis by using the independent muon data sample.

		efficiency%			
Source	Initial	Muon	$H_{\rm CAL}$	Muon *and* $H_{\rm CAL}$	Correlation factor
	1991-92				
τ pair MC	30399	86.5 $\pm$ 0.2	90.5 $\pm$ 0.2	79.2 $\pm$ 0.2	1.012 $\pm$ 0.005
Muon-pair data	22746	88.1 $\pm$ 0.2	85.0 $\pm$ 0.2	75.7 $\pm$ 0.3	1.011 $\pm$ 0.006
Muon-pair MC	86921	87.4 $\pm$ 0.1	85.7 $\pm$ 0.1	75.4 $\pm$ 0.2	1.007 $\pm$ 0.003
2-γ muon data	1474	88.3 $\pm$ 0.8	92.5 $\pm$ 0.7	84.1 $\pm$ 1.0	1.029 $\pm$ 0.026
2-γ muon MC	1308	86.9 $\pm$ 0.9	94.8 $\pm$ 0.6	83.3 $\pm$ 1.0	1.011 $\pm$ 0.026
	1993				
τ pair MC	29773	89.0 $\pm$ 0.2	89.6 $\pm$ 0.2	80.5 $\pm$ 0.2	1.010 $\pm$ 0.005
Muon-pair data	13125	89.9 $\pm$ 0.3	86.0 $\pm$ 0.3	78.1 $\pm$ 0.4	1.010 $\pm$ 0.008
Muon-pair MC	88650	90.0 $\pm$ 0.1	85.6 $\pm$ 0.1	77.5 $\pm$ 0.1	1.006 $\pm$ 0.003
2-γ muon data	778	91.1 $\pm$ 1.0	92.7 $\pm$ 0.9	86.4 $\pm$ 1.2	1.023 $\pm$ 0.035
2-γ muon MC	9970	88.0 $\pm$ 0.3	93.9 $\pm$ 0.2	83.3 $\pm$ 0.4	1.008 $\pm$ 0.009
	1994				
τ pair MC	120369	89.3 $\pm$ 0.1	89.5 $\pm$ 0.1	80.9 $\pm$ 0.1	1.012 $\pm$ 0.003
Muon-pair data	33795	89.7 $\pm$ 0.2	85.7 $\pm$ 0.2	77.7 $\pm$ 0.2	1.010 $\pm$ 0.005
Muon-pair MC	259043	91.7 $\pm$ 0.1	85.3 $\pm$ 0.1	78.7 $\pm$ 0.1	1.007 $\pm$ 0.002
2-γ muon data	2189	88.6 $\pm$ 0.7	91.9 $\pm$ 0.6	83.9 $\pm$ 0.8	1.030 $\pm$ 0.021
2-γ muon MC	11578	89.6 $\pm$ 0.3	93.9 $\pm$ 0.2	85.1 $\pm$ 0.3	1.011 $\pm$ 0.009

Table 4: The efficiencies for, and correlation factors between, the two $\tau \to \mu\nu\bar{\nu}$ selections for several sources using data from each year.

	91-92	93	94
N^{τ}_{Cand}	31201	20759	48782
$N^{\tau\to\mu\nu\bar{\nu}}_{Cand}$	4777	3287	7647
$f^{\tau}_{Bkgd}(\%)$	1.10 ± 0.16	1.21 ± 0.18	1.09 ± 0.29
$f^{\tau\to\mu\nu\bar{\nu}}_{Bkgd}(\%)$	2.65 ± 0.37	2.31 ± 0.45	2.49 ± 0.29
$\epsilon^{\tau\to\mu\nu\bar{\nu}}(\%)$	89.54 ± 1.28	90.78 ± 1.56	89.41 ± 1.01
$F^{\tau\to\mu\nu\bar{\nu}}_{Bias}$	0.9800 ± 0.0012	0.9806 ± 0.0012	0.9800 ± 0.0009
$B(\tau \to \mu\nu\bar{\nu})$ (%)	$17.18 \pm 0.22 \pm 0.07$	$17.59 \pm 0.27 \pm 0.09$	$17.64 \pm 0.18 \pm 0.08$

Table 5: Summary of the number of τ pair and $\tau \to \mu\nu\bar{\nu}$ candidates, background fractions, corrected efficiencies, selection biases and final branching ratio measurements for each year.

	Contributions to absolute error		
	1991-2	1993	1994
Statistical	0.215	0.268	0.175
Efficiency	0.018	0.018	0.012
f^{τ}_{Bkgd}	0.027	0.031	0.052
$f^{\tau\to\mu\nu\bar{\nu}}_{Bkgd}$	0.064	0.081	0.053
$F^{\tau\to x\nu\bar{\nu}}_{Bias}$	0.021	0.022	0.016
Total	0.228	0.283	0.191

Table 6: Breakdown of the contributing errors on the measured branching ratios for $\tau \to \mu\nu\bar{\nu}$ for each year's data expressed as an absolute error on the branching ratio when expressed in % .

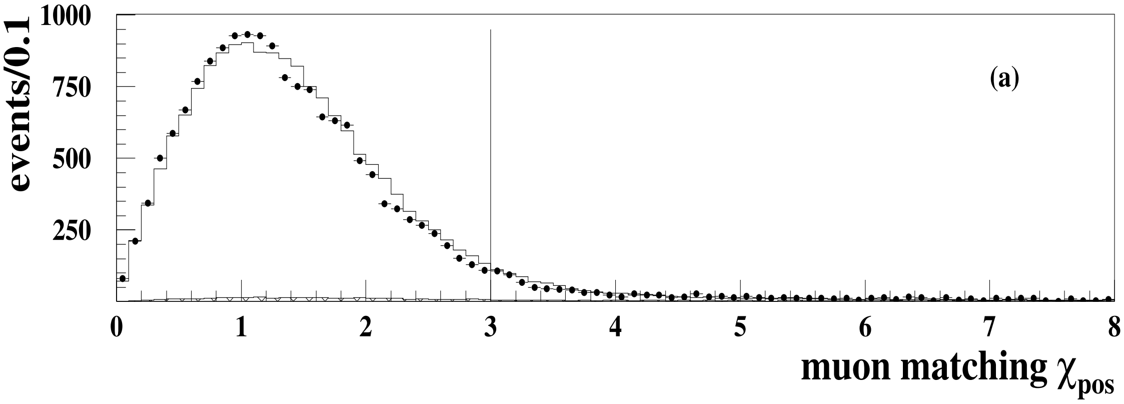

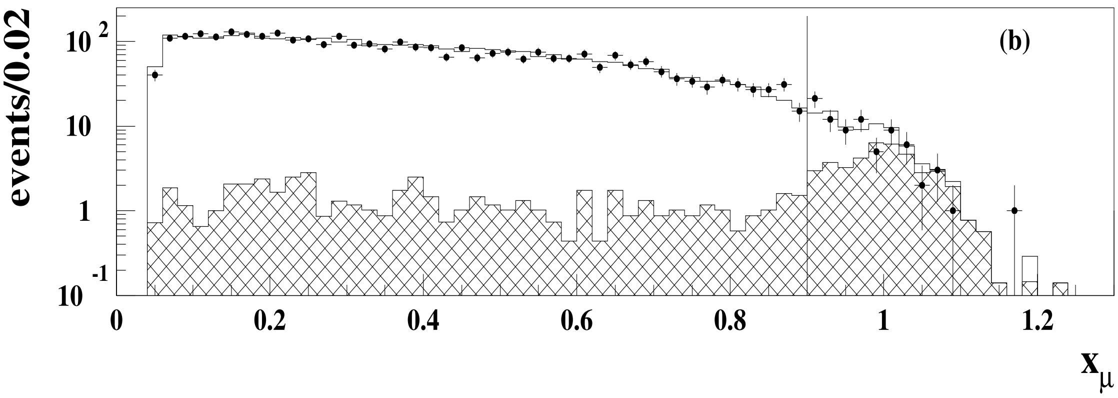

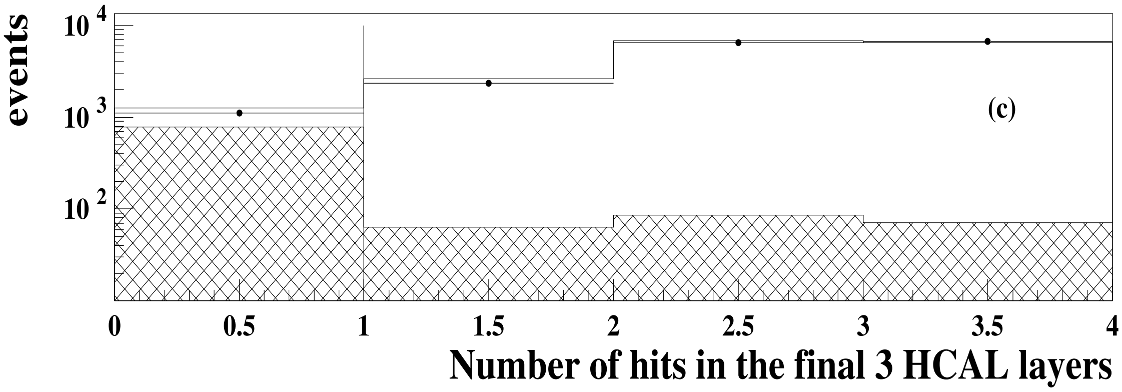

Figure 1: (a) The positional separation variable $\chi_{\rm pos}$ for the match between tracks in the jet chambers and activity in the muon layers. (b) The distribution of x_μ , as defined in Section2.2. for the nearside cones passing the muon chamber selection, given that the farside cone has $x_\mu > 0.9$. (c) The number of hits registered in the last three active layers of the hadron calorimeter in cones passing the hadron calorimeter selection. In this figure the points with error bars represent the data and the open(shaded) histogram the total(background) Monte Carlo prediction after all other cuts.

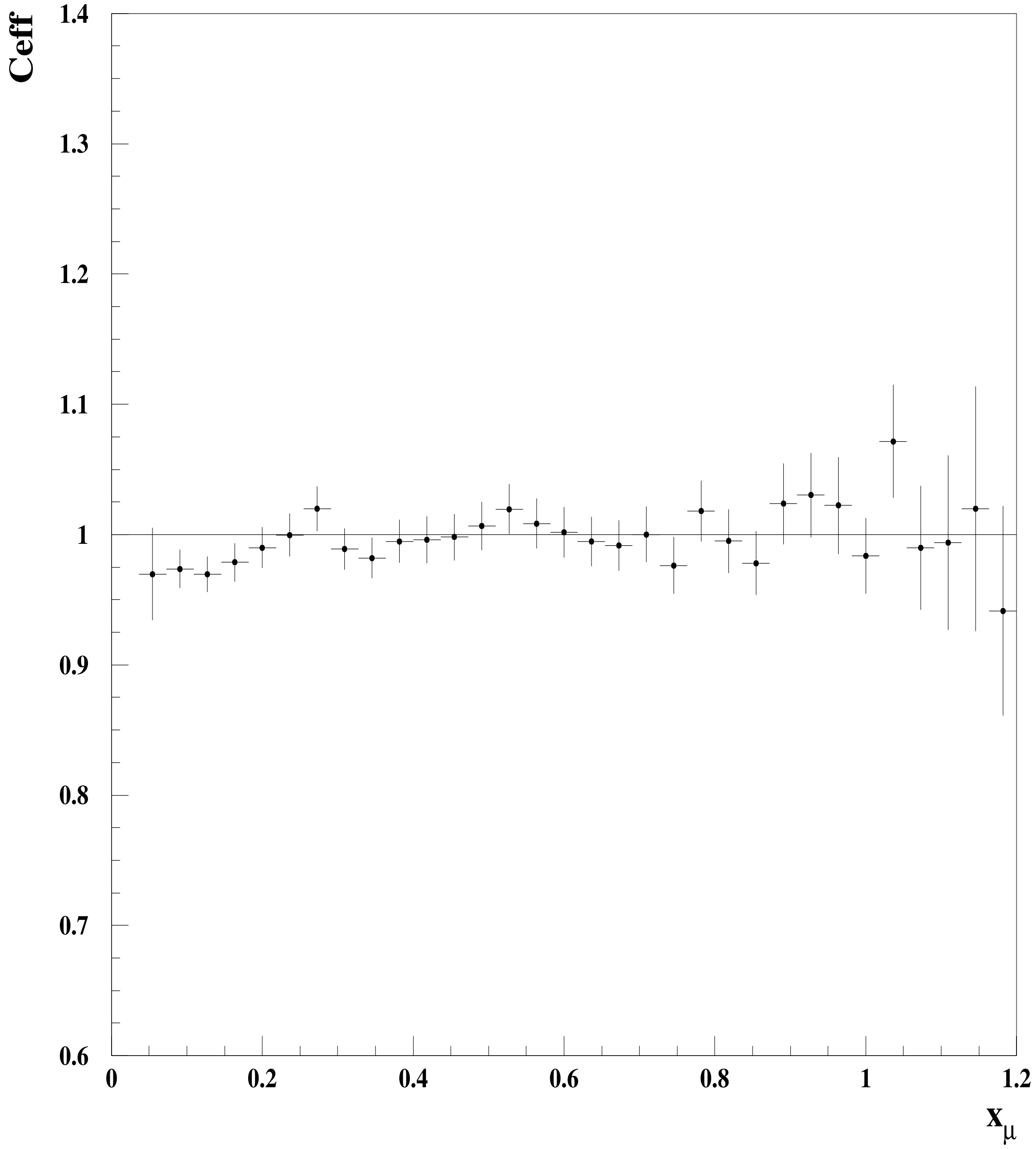

Figure 2: The efficiency correction factor $C_{\rm eff}$ as a function of x_μ as determined from the complete data and Monte Carlo samples as discussed in Section 3.2.

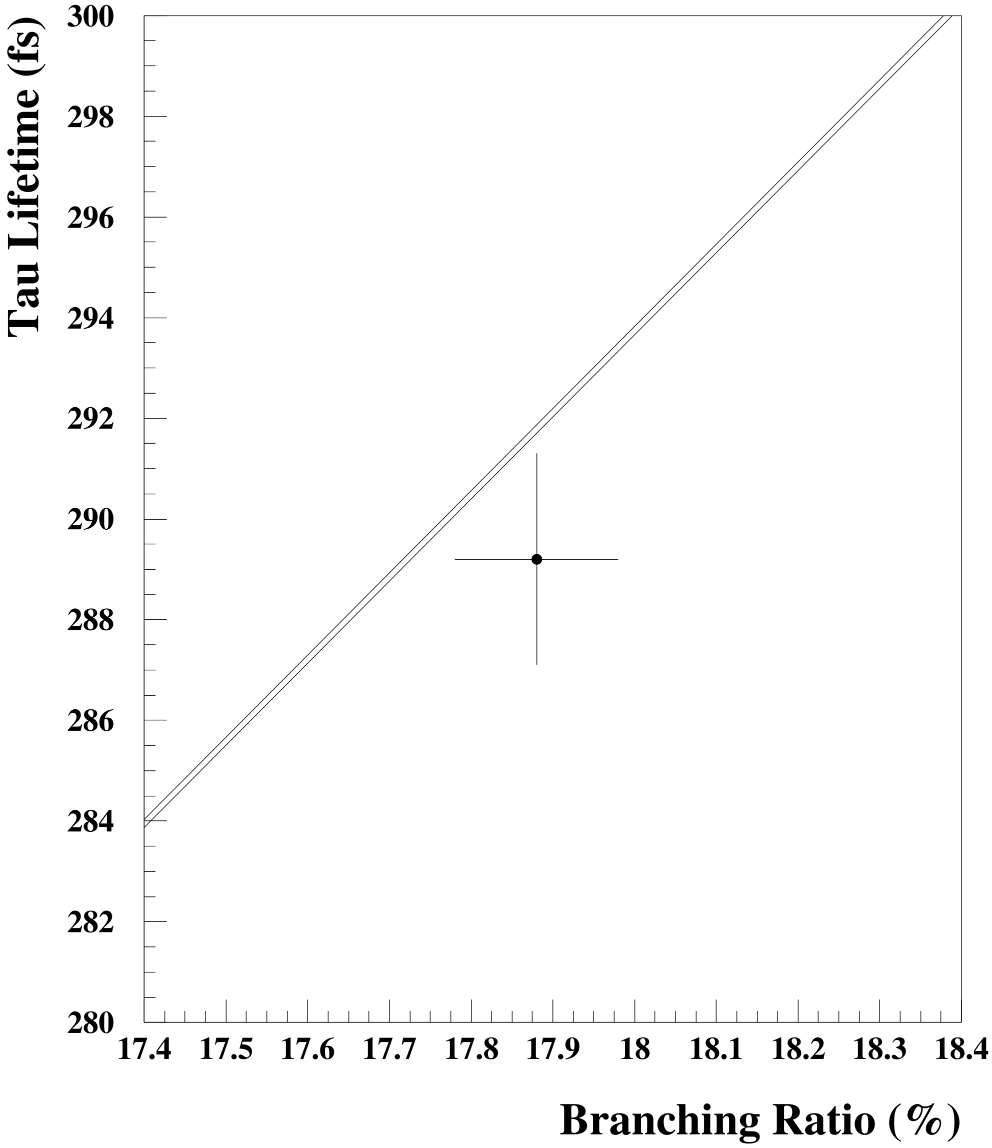

Figure 3: The average electronic branching ratio of the tau is plotted against the OPAL tau lifetime. The band is the prediction assuming $\mu - \tau$ universality and its width reflects the uncertainty associated with the tau mass.